Supplement of Biogeosciences Discuss., 12, 2213–2255, 2015
http://www.biogeosciences-discuss.net/12/2213/2015/
doi:10.5194/bgd-12-2213-2015-supplement

Biogeosciences
Discussions
Open Access

Supplement of

The dynamic of annual carbon allocation to wood in European forests is consistent with a combined source-sink limitation of growth: implications for modelling

J. Guillemot et al.

Correspondence to: J. Guillemot (joannes.guillemot@gmail.com)

Supplement

S1. Site description

A complete description of the 49 sites used in the study is available in Table S1.

Table S1 (next two pages)**.** Description of the studied sites.

ID letters indicate species (*F*: *Fagus sylvatica* ; *Qr* : *Quercus robur*, *Qp* : *Quercus petraea*, *P* : *Picea abies*, *Qi* : *Quercus ilex*). Lat.: Latitude, Long. : Longitude, Elev. Elevation, Exp.: Exposure, LNC: leaf nitrogen content ($gN.gDM^{-1}$), SWC: soil water holding capacity, H: dominant height in 1994, LAI: leaf area index (unitless), ETP: potential evapotranspiration (calculated using the Penman-Monteith equation on a daily basis) , Prec.: precipitation, T: temperature, SNA: soil nutrient availability classes (1=high, 2=medium, 3=low nutrient availability), period: dates and number of available AWBI measurements. ETP, Prec. and T are averaged annual values.

ID	Lat. (N)	Long. (E/W)	Elev. (m)	Slope %	Exp.	LNC	Age (year)	SWC (mm)	H (m)	LAI	ETP (mm)	Prec. (mm)	T (°C)	SNA	period (nb. of years)
F 03	46° 11’	2° 59’ E	590	15	N	28.3	87	155	29	6.6	1079	778	10.5	2	1994-1970 (25)
F 04	44° 07’	5° 47’ E	1300	50	N	26.7	85	180	25.5	6.6	1328	917	11.6	1	1994-1983 (12)
F 09	42° 55’	1° 16’ E	1250	32	SW	26.3	152	110	21.8	4.6	1069	1068	11.5	3	1994-1964 (31)
F 14	49° 10’	0° 51’W	90	0	-	25.3	83	83	25.7	6.2	859	892	10.8	3	1994-1976 (19)
F 21	47° 48’	4° 51’ E	400	3	NE	23.5	128	80	28.6	4.3	966	934	9.7	1	1994-1975 (20)
F 26	44° 55’	5° 17’ E	1320	12	W	28.3	158	80	80	4.3	1106	1364	6.8	1	1994-1973 (22)
F 52	47° 47’	5° 04’ E	440	0	-	25.2	106	100	30.2	5.9	947	987	9	1	1994-1973 (22)
F 54a	48° 30’	6° 42’ E	325	5	E	27.1	95	120	29.1	6.2	888	1038	9.5	3	1994-1972 (23)
F54b	48° 38’	6° 04’ E	390	2	-	26.3	99	60	28.3	6.2	885	823	9.8	1	1994-1981 (14)
F 55	49° 11’	5° 00’ E	250	0	-	25.8	88	150	29.4	5.9	1000	965	9.6	3	1994-1980 (15)
F 60	49° 19’	2° 52’ E	138	0	-	26.6	62	160	26.8	6.6	920	717	10.1	2	1994-1982 (13)
F 64	43° 08’	0° 39 W	400	44	NW	26	67	137	28.8	5.3	1064	1299	12.7	2	1994-1977 (18)
F 65	43° 01’	0° 26’ E	850	25	NW	29.1	160	180	180	6.4	1080	1114	11.6	2	1994-1972 (23)
F 76	49° 42’	1° 19’ E	210	0	-	24.5	87	90	29.9	6.5	776	930	9.9	2	1994-1974 (21)
F 81	43° 24’	2° 10’ E	700	0	-	28.1	108	140	30.3	6.3	1219	1102	9.9	2	1994-1972 (23)
F 88	48° 06’	6° 14’ E	400	3	W	27.5	68	100	25.4	5.9	877	1092	9.1	3	1994-1983 (12)
Qr 77	48° 27’	2° 42’ E	80	0	-	24.3	113	150	27.8	6.1	1009	719	10.7	2	1994-1985 (10)
Qr 18	46° 49’	2° 34’ E	175	2	NW	26.9	58	180	17.7	4.6	1031	782	11	2	1994-1987 (8)
Qr 40	43° 44’	0° 50’ W	20	5	NE	25.2	46	140	25	5.6	1049	1010	13	1	1994-1984 (11)
Qr 49	47° 27’	0° 01’W	57	0	-	29.1	70	170	28.1	6.9	1085	665	11.5	1	1994-1983 (12)
Qr 55	49° 01’	5° 45’ E	220	0	-	23.9	100	150	20.1	5.9	929	827	9.4	1	1994-1972 (23)
Qr 59	50° 10’	3° 45’ E	149	3	-	27.2	70	200	22.8	6.5	986	870	9.8	1	1994-1974 (21)
Qr 65	43° 12’	0° 02’ W	370	12	SE	25.5	54	160	24.9	4.7	1042	965	12	1	1994-1986 (9)
Qr 71	46° 58’	5° 14’ E	190	0	-	26.3	67	190	25.6	6.5	1096	1006	11.3	1	1994-1972 (23)
Qp 01	46° 10’	5° 14’ E	260	3	-	23.7	88	170	25.9	6.5	1015	1017	10.5	1	1994-1982 (13)
Qp 03	46° 40’	2° 43’ E	260	0	-	27.4	115	100	30.5	5.6	1080	802	10.5	2	1994-1965 (30)
Qp 10	48° 17’	4° 27’ E	160	0	-	22.9	83	200	24.9	6.3	1010	778	10.4	1	1994-1987 (8)
Qp 18	47° 15’	2° 07 W	176	1	-	26.3	78	150	28.2	5.9	1025	792	10.9	2	1994-1978 (17)
Qp 27	49° 21’	1° 03’ E	175	0	-	27.2	55	170	23.4	6.5	844	768	9.8	2	1994-1984 (11)
Qp 35	48° 10’	1° 32’ W	80	0	-	26.3	101	120	29.3	6.1	893	764	11	2	1994-1966 (29)
Qp 41	47° 34’	1° 15’ E	127	0	-	25.6	92	180	28.1	5.9	985	639	10.9	3	1994-1972 (23)
Qp 51	49° 01’	4° 57’ E	180	2	S	25.4	139	80	25.2	5.9	969	877	9.9	3	1994-1964 (31)
Qp 57a	48° 52’	6° 28’ E	320	4	NE	25.1	85	150	27.7	5	1009	719	10.7	1	1994-1970 (25)
Qp 57b	49° 00’	7° 27’ E	320	15	NW	20.9	128	140	28.7	5.6	1009	719	10.7	3	1994-1964 (31)
Qp 58	46° 58’	3° 39’ E	270	7	SW	24.1	66	150	23.5	6.2	1088	928	10.8	2	1994-1983 (12)
Qp 60	49° 23’	2° 17 W	55	1	-	26.5	60	140	25.3	6.5	855	674	10.2	1	1994-1979 (16)
Qp 61	48° 31’	0° 40’ E	220	5	SE	25.8	88	110	26.9	6.7	889	773	10.1	2	1994-1981 (14)
Qp 68	47° 41’	7° 28’ E	256	0	-	27.9	137	80	22	5.6	891	811	10.1	3	1994-1970 (25)
Qp 72	47° 46’	0° 22’ E	170	0	-	22	64	170	24.1	5.9	952	719	10.9	3	1994-1987 (8)
Qp 81	44° 02’	1° 44’ E	300	18	SE	22.1	98	100	27.8	5.3	1246	869	12.0	2	1994-1972 (23)
Qp 86	46° 37’	0° 29’ E	116	4	NW	24	82	80	25.1	6.0	1121	758	11.5	3	1994-1985 (10)
Qp 88	48° 01’	6° 02’ E	330	0	-	24.8	129	200	26.4	5.7	877	1103	8.99	2	1994-1964 (31)

Table S1. *Continued*

ID	Lat. (N)	Long. (E/W)	Elev. (m)	Slope %	Exp.	LNC	Age	SWC (mm)	H (m)	LAI	ETP (mm)	Prec. (mm)	T (°C)	SNA	period (nb. of years)
P 39a	46° 11’	2° 59’ E	970	10	SE	14	58	90	30.4	6.9	942	1865	7.5	1	1994-1973 (22)
P 39b	44° 07’	5° 47’ E	1210	8	W	12.9	111	80	23.6	5.4	931	2100	5.7	1	1994-1979 (16)
P 71	42° 55’	1° 16’ E	600	20	SE	13.1	48	100	27	5.8	1055	936	9.8	3	1994-1980 (15)
P 73	49° 10’	0° 51’W	1700	40	NW	12.7	182	110	22.7	4.2	869	1263	4.1	2	1994-1979 (16)
P 74	47° 48’	4° 51’ E	1200	20	W	13.8	73	150	30	8.4	939	1737	7.2	2	1994-1978 (17)
P 88	44° 55’	5° 17’ E	660	20	SW	14.2	89	100	35.5	6.1	867	1458	8.5	2	1994-1980 (15)
Qi 34	43° 44’	3° 35’ E	270	0	-	12	68	113	6	2.4	1417	907	13.4	-	2008-1966 (43)

S2. Reconstruction of the historical circumference trajectories

The historical circumference (CBH) trajectories were obtained on the 49 studied plots by combining forest inventories and tree-ring series. Dendrochronological sampling was conducted after the completion of the forest inventories (Figure S1), so that the calculation of historical CBHs inventories could rely on tree-ring series information. 30 trees were cored in the RENECOFOR network (Lebourgeois 1997) and 12 were cored in the Puechabon site (J.M. Limousin, *unpublished data*). Past CBH was annually calculated from the initial forest inventory backward. Reconstruction stopped when a sharp decrease of CBH growth indicated non-reported past silvicultural intervention or when the associated stand age felt below 25 years (Figure S1).

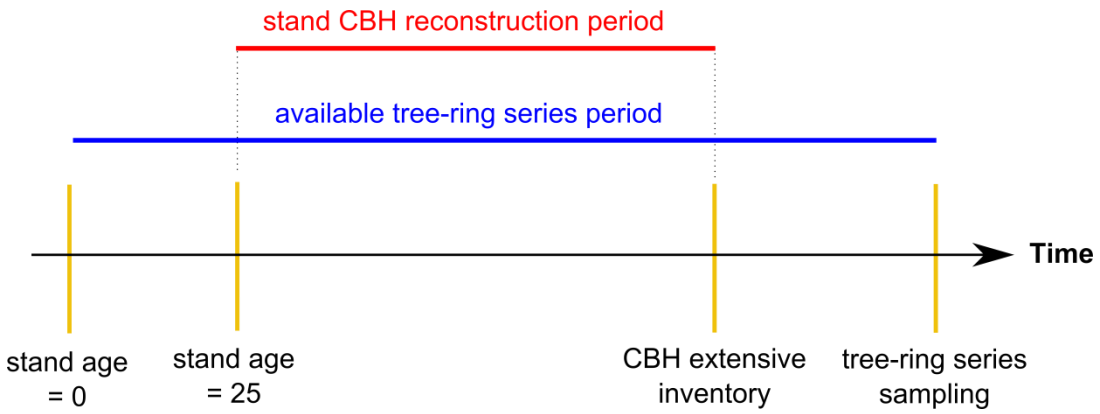

Figure S1. Illustration of the growth measurement timing.

First, the CBH trajectories of the cored trees were calculated using tree rings and the CBHs measured at the sampling time. Annual basal area increments were then calculated as follows.

$$BAI_{t,i} = \frac{1}{4\pi}\left(CBH_{t,i}{}^2 - CBH_{t,i-1}{}^2\right) \quad \text{(Eq. S1)}$$

where $BAI_{t,i}$ is the basal area increment observed on a tree t, in a year i.

In a second step, BAI and CBH data were used to calibrate – for each year and each plot - an empirical tree competition model (Deleuze *et al.* 2004), following the approach described in (Guillemot *et al.* 2014). The considered model can be written as follows.

$$BAI_{t,i} = \frac{\gamma_i}{2} \times (CBH_{t,i} - m\sigma_i + \sqrt{(m\sigma_i + CBH_{t,i})^2 - 4\sigma_i \times CBH_{t,i}}) \quad \text{(Eq. S2)}$$

where $CBH_{t,i}$ is the circumference at breast height of a given tree t in a year I, and $BAI_{t,i}$ is its corresponding annual basal area increment. σ and γ are the annually calibrated parameters. In this model, only trees with a circumference at breast height (CBH) above the threshold σ_i, which can be interpreted as the minimum circumference for direct access to sunlight, have a significant growth. Overstory trees then grow proportionally to their sizes, following a slope coefficient γ_i (Fig. S2). *m* is a smoothing parameter.

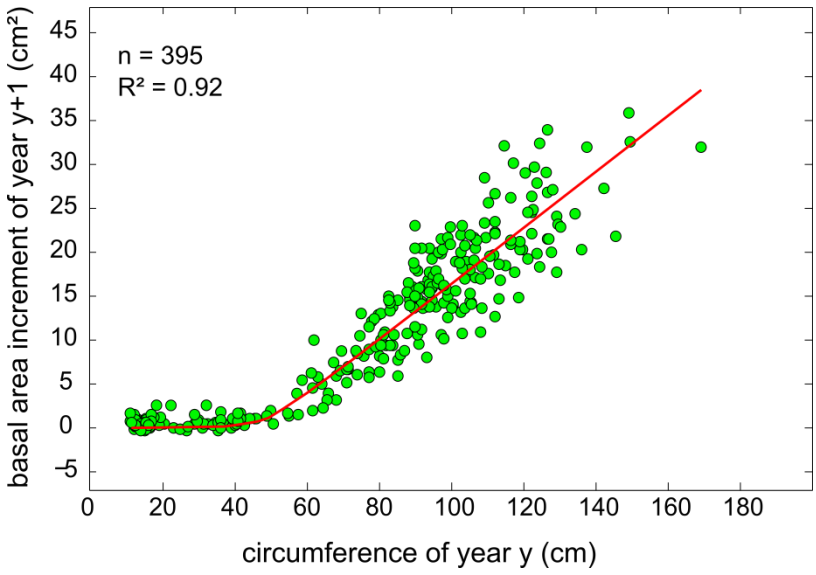

Figure S2. Illustration of the tree competition model described in Eq. S2. Data were obtained from extensive inventories lead in 2000 and 2009 in plot *F*03 (Guillemot *et al.* 2014).

The calibrated model was then used to infer the BAIs of all the trees of the initial CBH stand distribution. The whole calculation followed an algorithm displayed in Figure S3.

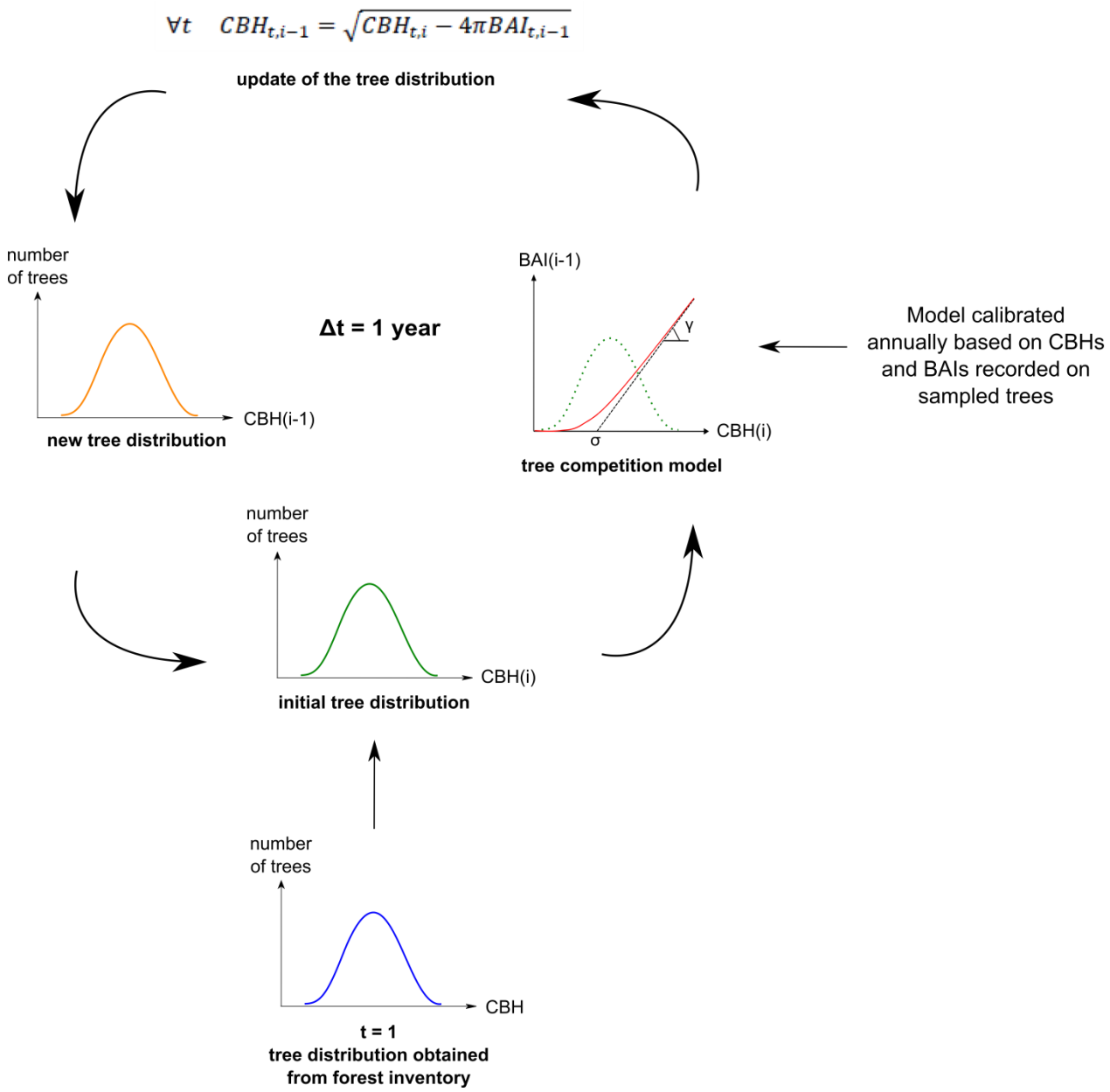

Figure S3. Illustration of the algorithm used to reconstruct historical circumference trajectories.

S3. Functions used in the calculation of woody biomass

Tree woody biomass calculation was based on distinct procedure for *F. sylvatica*, *Q. petraea* and *P. abies* on one hand, and *Q. ilex* on other hand.

S3.1. *F. sylvatica*, *Q. petraea* and *P. abies*

- **Top height**

- *F. sylvatica* curves

We used the curves suggested by Bontemps, Hervé & Dhôte (2009) which account for the long-term forest productivity trend induced by global changes. The dominant height at the age t, H_t (m), is described as follows.

$$H_t = m1.\exp\left(-\left(pf.m2.chprod(date_0 + t) + \left(ln\left(\frac{a}{H_{t-1}}\right)\right)^{-\frac{1}{m3}}\right)^{-m3}\right) \qquad \text{(Eq. S3)}$$

with

$$\begin{cases} if\ 1900 < date < 2000\ then\ chprod(date) = 1 + m4.(date - 1900) + m5.(date - 1900)^2 \\ if\ date \leq 1900\ then\ chprod(date) = 1 \\ if\ date \geq 2000\ then\ chprod(date) = chprod(2000) \end{cases}$$

- *Q. petraea* curve

Similarly, the curve suggested by Bontemps *et al.* (2012) also includes explicitly the changes in forest productivity.

$$\frac{dH}{dt} = f2(t - t_b).p_f.f1(H) \qquad \text{(Eq. S4)}$$

where *H* is the top height (m), t is date, tb is a reference date (here t_b=1900).

$$f1(H) = \frac{(\frac{H}{K_S})^{m1.m2}}{(1 - m1 + m1(\frac{H}{m3})^{m2})} \qquad \text{(Eq. S5)}$$

$f2(t) = 1 + d1.u + d2.u^2 + d3.u^3 + \sum_{k=1}^{4} p_k.max(u - 20.k, 0)^3 + \sum_{k=0.}^{1} pm_k.min(u - 20.k, 0)^3$ (Eq. S6)

with $u = t - 1900$

Equation S4 was integrated numerically using Range-Kutta 4 method.

- *P. abies* curve

We used the curve suggested in Seynave *et al.* (2005).

$$H_{age} = m1.\exp\left(-\frac{\left(age.p_f.exp\left(\left(1+\frac{1}{m2}\right).\left(1-ln\left(1+\frac{1}{m2}\right)\right)\right)\right)}{\left((m1.m2)+\left(ln\left(\frac{m1}{1.3}\right)\right)^{\frac{-1}{m2}}\right)^{-m2}}\right) \quad \text{(Eq. S7)}$$

where H_{age} is the stand dominant height (m) at the corresponding age.

- Parameterization and initialization

The parameterization of Eq. S3, S4 and S7 are provided in Table S2.

Table S2. Parameterization of the top height models

Species		Parameter values
F. sylvatica	Eastern France	m1=68.7; m2=0.028; m3=0.823; m4=$2.03.10^{-3}$; m5=$3.96.10^{-5}$
	Western France	m1=44.2; m2=0.032; m3=1.647; m4=$1.245.10^{-3}$; m5=$1.74.10^{-5}$
Q. petraea		K_s=6.1; m1=0.138; m2=2.36; d1=$0.2.10^2$; d2=$0.027.10^3$; d3=-$0.063.10^4$; p1=$0.284.10^4$; p2=-0.622; p3=1.076; p4=-1.545; pm0=0.024; pm1=-0.076
P. abies		m1=50.7; m2=1.08

F. sylvativa and *Q. petraea* curves require initialization, defined as follows: $H_{age=0} = 0.3m$.

The parameter p_f in Eq. S3, S4 and S7 is the site-specific fertility parameter. p_f values have been defined by calibrated the curves on height and age measurements. The resulting curves are displayed in Figure S4.

- **Individual height**

The height of each tree is then calculated using the hyperbolic model suggested by Dhôte and de Hercé (1994):

$$H = 1.3 + \frac{((H_0 - 1.3 + p_2.CBH) - \sqrt{H_0 - 1.3 + p_2.CBH)^2 - 4.p_3.p_2.(H_0 - 1.3).CBH}}{2.p_3} \quad \text{(Eq. S8)}$$

where H is the height of a given tree with a circumference CBH and H_0 is the stand dominant height.

p_2 and p_3 parameters were defined per plot using height and CBH measurements.

- **Individual above-ground volume equations**

Tree above-ground volumes were calculated from CBH and H, using the equations established by Vallet et al. (2006):

$$V = form \frac{1}{40000\pi} CBH^2.H \quad \text{(Eq. S9)}$$

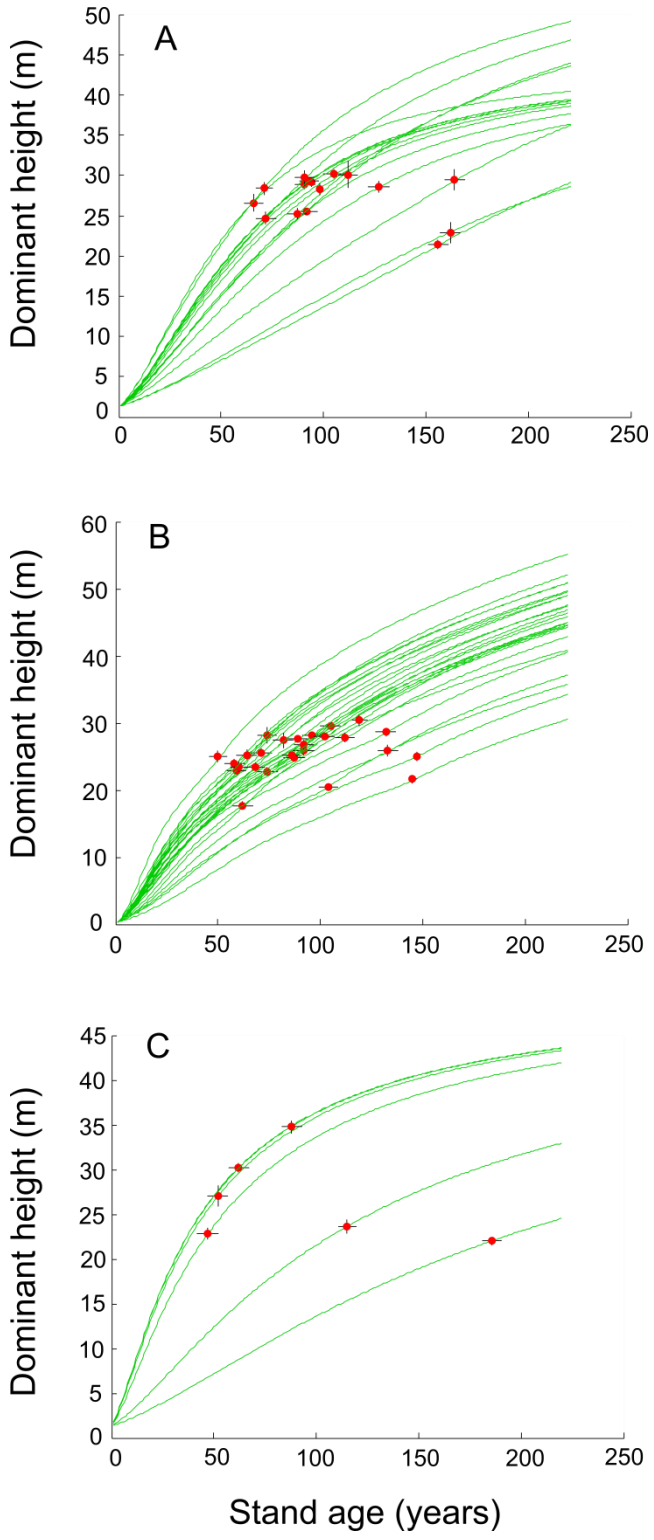

Figure S4. Site-specific top height curves for *F. sylvatica* (A), *Q. petraea* (B) and *P. abies* (C). Points and error bar correspond to age and height measurements.

where

V is the total above ground tree volume and

$form = (\alpha + \beta . CBH + \gamma . hdn)(1 + \frac{\delta}{CBH^2})$ (Eq. S10)

with hdn = $CBH^{1/2}$ / H.

Parameterization of eq. (S9) and (S10) is provided in Table S3.

Table S3. Parameterization of the tree volume equations

Parameter	*Q. petraea*	*F. sylvatica*	*P. abies*
α	0.471	0.395	0.631
β	-0.000345	0.000266	-0.000946
γ	0.377	0.421	0
δ	0	45.4	0

- **Wood density models**

Wood density models typically relates the density of a tree ring formed in year i (WD_i) to tree age (age_i) and ring width (RW_i) (Guilley, Hervé & Nepveu 2004; Bergès, Nepveu & Franc 2008).

We used density models established by:

- Zhang et al. (1993) for *Q. petraea*, with WD models as

$$WD_i = \frac{a + b.age_i - (\frac{c}{RW_i}) - (\frac{d.age_i}{RW_i})}{1.235}$$ (Eq. S11)

- Bouriaud et al. (2004) for *F. sylvatica*, with

$$WD_i = \frac{a - b.age + \frac{c}{RW_i}}{1.3}$$ (Eq. S12)

- Wilhelmsson *et al.* (2002) for *P. abies*

$$WD_i = a + e.(\ln(age))^b - c.\frac{RW_i}{age \times T_{sum}} + \frac{d.Tsum}{\frac{1}{2}.\frac{RW_i}{age} + 2.3}$$ (Eq. S13)

with

T_{sum} =4922.1-60.367*48-0.837*1000

Parameterization of equations S11, S12 and S13 is provided in Table S4.

Table S4. Parameterization of the wood density models

Parameter	Q. petraea	F. sylvatica	*P. abies*
a	817.9	789	304.3
b	0.0038	0.86	0.5
c	98.927	0.32	-444.13
d	0.922	-	0.295
e	1.235	1.3	10.4437

Annual wood density was calculated for all the available dendrochronological tree ring series and use to convert the corresponding annual volume increment in annual dry matter increment. The dry matter mass was then converted to carbon biomass assuming 50% carbon content in woody tissues (Pignard *et al.* 2000).

- **Individual total volume calculation**

Total tree woody biomass of all sites was obtained from above-ground biomass using age-related species-specific relationship after checking for no additional effect of stand density and mean tree size (data not shown).

$$TWB = AWB + AWB \times RS(age)$$

with TBW the total woody biomass, AWB the above-ground woody biomass and RS the root-shoot ratio, function of stand age.

We used root-shoot model established by Genet, Bréda & Dufrêne (2010) for *Q. petraea and F. sylvatica* and Lehtonen *et al.* (2004) for *P. abies*.

$$RS(age) = a + b.\exp(c \times age)$$ (Eq. S14)

Table S5. Parameterization of the root-shoot models

Parameter	*Q. petraea*	*F. sylvatica*	*P. abies*
a	0.1893	0.183	0.0838
b	0.8295	1.6259	-0.0365
c	-0.0496	-0.3174	-0.01

S3.2. *Q. ilex*

The calculation of AWB for Q. ilex benefited from the work of Rambal *et al.*(2004) conducted on the studied plot (Puechabon site). AWB_i of a given tree i was related directly to CBH_i using a relationship calibrated on 10 stems.

$$AWB = 191.6 \times \left(\frac{CBH}{\pi}\right)^{2.171}$$ (Eq. S15)

The Puechabon site is managed as a coppice, with *Q. ilex* stems sprouting from the stumps after cutting. For this reason, root biomass is there much more important than shoot biomass, at least during the first part of the coppice rotation. We assumed consequently no root biomass growth over the studied period in this site and we calculated the corresponding annual woody biomass increments directly from AWB and not from TWB.

S4. Annual woody biomass increment features

We calculated annual woody biomass increments as follows for the RENECOFOR plots.

$$AWBI_i = TWB_i - TWB_{i-1}$$ (Eq. S16)

where i corresponds to year.

For the Puechabon site, AWBIs were calculated as follows.

$AWBI_i = AWB_i - AWB_{i-1}$ (Eq. S17)

Characteristics of the calculated AWBIs are presented in Table S6. The mean sensitivity and first order auto-correlation coefficient were calculated on detrended data to measure, respectively, the year-to-year variability and the lagged influence of growth of the previous year on the current year growth (Fritts 2012).

Table S6. Site-specific characteristics of the annual woody biomass increments (AWBI). R^2 and RMSE (coefficient of determination and root mean square error) correspond to the goodness of fit of the tree competition model used in the CBH reconstruction (mean ±.standard error), mean AWBI is calculated on raw data, MS and AC are the mean sensitivity and the first-order autocorrelation coefficient of the detrended AWBI series, respectively.

ID	R^2 (%)	RMSE ($gC.m^{-2}$)	mean AWBI ($gC.m^{-2}$)	MS (unitless)	AC (unitless)
F 03	*36.8 ± 3.9*	*10.0 ± 1.3*	*379.7*	*0.19*	*0.40*
F 04	*61.6 ± 14.3*	*5.1 ± 2.3*	*267.0*	*0.17*	*0.15*
F 09	*52.0 ± 13.9*	*9.8 ± 0.9*	*158.7*	*0.22*	*0.18*
F 14	*54.2 ± 14.4*	*5.4 ± 1.9*	*262.8*	*0.23*	*0.36*
F 21	*35.0 ± 5.9*	*13.3 ± 1.9*	*204.5*	*0.23*	*0.36*
F 26	*54.0 ± 11.6*	*9.3 ± 0.6*	*160.1*	*0.22*	*0.28*
F 52	*41.6 ± 12.5*	*5.5 ± 1.6*	*273.7*	*0.26*	*0.18*
F 54a	*60.7 ± 16.1*	*9.7 ± 2.4*	*391.1*	*0.23*	*0.16*
F54b	*67.1 ± 11.5*	*7.7 ± 1.9*	*231.3*	*0.21*	*0.29*
F 55	*46.9 ± 17.8*	*9.9 ± 2.0*	*379.0*	*0.12*	*0.20*
F 60	*74.1 ± 18.1*	*6.3 ±1.6*	*405.7*	*0.17*	*0.32*
F 64	*52.4 ± 13.1*	*8.4 ± 2.3*	*415.1*	*0.17*	*0.34*
F 65	*59.3 ± 12.2*	*7.3 ± 1.3*	*237.9*	*0.15*	*0.24*
F 76	*36.5 ± 9.9*	*8.8 ± 1.8*	*278.2*	*0.19*	*0.41*
F 81	*38.8 ± 13.3*	*7.5 ± 1.5*	*279.9*	*0.18*	*0.37*
F 88	*38.9 ± 5.3*	*6.7 ± 1.2*	*381.1*	*0.13*	*0.45*
Qr 77	*42.6 ± 16.1*	*9.7 ± 2.4*	*238.7*	*0.15*	*0.67*
Qr 18	*68.6 ± 6.2*	*3.6 ± 1.3*	*247.2*	*0.17*	*0.20*
Qr 40	*63.5 ± 15.6*	*8.7 ± 1.7*	*351.9*	*0.18*	*0.26*
Qr 49	*44.5 ± 7.0*	*10.8 ± 1.7*	*409.3*	*0.13*	*0.46*
Qr 55	*30.7 ± 10.9*	*7.6 ± 1.8*	*104.0*	*0.15*	*0.23*
Qr 59	*38.0 ± 13.8*	*5.6 ± 1.6*	*228.3*	*0.22*	*0.20*
Qr 65	*77.8 ± 7.5*	*4.9 ± 1.3*	*296.5*	*0.23*	*0.24*
Qr 71	*35.4 ± 1.4*	*6.7 ± 1.6*	*303.4*	*0.17*	*0.25*
Qp 01	*47.0 ± 12.7*	*5.1 ± 1.5*	*264.2*	*0.15*	*0.12*
Qp 03	*70.8 ± 11.9*	*4.3 ± 0.9*	*278.7*	*0.14*	*0.17*
Qp 10	*34.8 ± 7.6*	*7.6 ± 1.6*	*260.9*	*0.12*	*0.28*
Qp 18	*37.9 ± 5.8*	*6.9 ± 1.8*	*370.4*	*0.15*	*0.33*
Qp 27	*87.4 ± 9.1*	*5.4 ± 1.5*	*303.3*	*0.14*	*0.16*
Qp 35	*35.0 ± 10.1*	*6.5 ± 1.5*	*307.4*	*0.12*	*0.22*
Qp 41	*61.8 ± 19.6*	*5.9 ± 0.8*	*276.6*	*0.19*	*0.31*
Qp 51	*73.5 ± 17.0*	*5.9 ± 0.9*	*184.1*	*0.13*	*0.39*
Qp 57a	*57.2 ± 13.9*	*3.8 ± 1.1*	*355.1*	*0.18*	*0.32*
Qp 57b	*77.8 ± 9.5*	*4.8 ± 0.6*	*175.5*	*0.13*	*0.28*
Qp 58	*64.2 ± 9.8*	*6.2 ±0.9*	*345.3*	*0.11*	*0.27*
Qp 60	*63.9 ± 10.3*	*4.7 ±1.1*	*344.9*	*0.19*	*0.15*
Qp 61	*41.9 ± 6.0*	*4.6 ±0.7*	*316.9*	*0.10*	*0.18*
Qp 68	*36.4 ± 4.5*	*7.5 ± 2.0*	*99.7*	*0.18*	*0.11*
Qp 72	*65.6 ± 9.7*	*4.8 ± 1.4*	*370.9*	*0.17*	*0.14*
Qp 81	*54.0 ± 22.4*	*3.7 ± 1.1*	*197.8*	*0.18*	*0.18*
Qp 86	*60.0 ± 11.3*	*6.2 ± 1.2*	*343.1*	*0.19*	*0.25*
Qp 88	*35.2 ± 13.1*	*5.7 ± 1.9*	*209.3*	*0.15*	*0.40*
P 39a	*36.2 ± 18.3*	*10.0 ±2.3*	*472.4*	*0.16*	*0.29*
P 39b	*46.6 ± 10.9*	*5.1 ± 0.9*	*236.2*	*0.14*	*0.32*
P 71	*47.8 ± 14.7*	*9.8 ± 2.5*	*318.5*	*0.20*	*0.34*
P 73	*69.8 ± 15.8*	*5.4 ± 0.8*	*207.8*	*0.15*	*0.31*
P 74	*45.2 ± 14.9*	*13.3 ± 2.0*	*475.7*	*0.16*	*0.35*
P 88	*63.8 ± 12.8*	*9.3 ± 1.6*	*365.6*	*0.13*	*0.31*
Qi 34	*59.3 ± 14.2*	*9.2 ± 1.2*	*101.9*	*0.35*	*0.12*

S5. Classes of soil nutrient availability

Table S7. Soil characteristics of the studied plots. C/N: carbon-nitrogen biomass ratio, T/S: percent base saturation, CEC: cationic exchange capacity, SNA: soil available nutrient classes (1=high, 2=medium, 3=low nutrient availability).

ID	C/N	T/S	CEC	SNA
F 03	*14.5*	*9.8*	*4.2*	2
F 04	*13.2*	*99.9*	*29.4*	1
F 09	*14.8*	*13.2*	*5.3*	3
F 14	*15.6*	*9.8*	*4.2*	3
F 21	*15.0*	*99.9*	*42.3*	1
F 26	*11.9*	*99.9*	*39.8*	1
F 52	*13.3*	*99.8*	*30.9*	1
F 54a	*15.0*	*19.9*	*3.4*	3
F54b	*12.6*	*99.7*	*38.3*	1
F 55	*17.7*	*11.9*	*3.0*	3
F 60	*13.0*	*99.9*	*13.7*	2
F 64	*10.5*	*60.7*	*6.6*	2
F 65	*11.3*	*10.5*	*5.3*	2
F 76	*13.7*	*9.0*	*3.3*	2
F 81	*14.2*	*12.9*	*4.4*	2
F 88	*16.2*	*12.6*	*3.8*	3
Qr 77	*14.8*	*34.8*	*1.05*	2
Qr 18	*17.8*	*88.6*	*14.5*	2
Qr 40	*11.6*	*73.8*	*2.75*	1
Qr 49	*10.7*	*39.1*	*1.2*	1
Qr 55	*12.9*	*86.0*	*15.3*	1
Qr 59	*12.7*	*42.1*	*6.5*	1
Qr 65	*10.2*	*26*	*2.8*	1
Qr 71	*14.6*	*54.0*	*4.4*	1
Qp 01	*12.8*	*13.5*	*2.8*	1
Qp 03	*16.8*	*23.9*	*1.5*	2
Qp 10	*13.6*	*23.2*	*5.8*	1
Qp 18	*19.5*	*11.8*	*1.4*	2
Qp 27	*14.9*	*20.1*	*6.3*	2
Qp 35	*15.2*	*7.7*	*2.8*	2
Qp 41	*17.8*	*16.2*	*3.8*	3
Qp 51	*19.7*	*25.9*	*6.7*	3
Qp 57a	*12.0*	*29.1*	*3.9*	1
Qp 57b	*23.6*	*7.5*	*2.0*	3
Qp 58	*14.9*	*29.3*	*3.4*	2
Qp 60	*13.4*	*36.9*	*2.6*	1
Qp 61	*15.8*	*31.3*	*6.8*	2
Qp 68	*16.1*	*21.9*	*3.5*	3
Qp 72	*25.3*	*11.9*	*2.9*	3
Qp 81	*15.9*	*23.2*	*6.2*	2
Qp 86	*26.0*	*12.0*	*2.4*	3
Qp 88	*15.9*	*20.8*	*4.5*	2
P 39a	*10.9*	*98.1*	*26.8*	1
P 39b	*10.9*	*98.1*	*26.8*	1
P 71	*12.3*	*4.5*	*4.0*	3
P 73	*15.7*	*34.5*	*4.0*	2
P 74	*12.4*	*98.1*	*14.1*	2
P 88	*15.3*	*14.3*	*4.0*	2
Qi 34	-	-	-	-

S6. Seasonal agreement between AWBIs and the components of the forest carbon balance

Figure S5 (next two pages). Seasonal agreement between AWBIs and the components of the forest carbon balance.

Values are the median of the Pearson coefficients estimated on each plot. Triangle marks the maximum median value. Critical values for each flux (G: gross primary productivity, N: net primary productivity, R: autotrophic respiration) are reported with arrows on the color-bar. Critical values outside the color-bar mean that no values differed from the maximum median correlation.

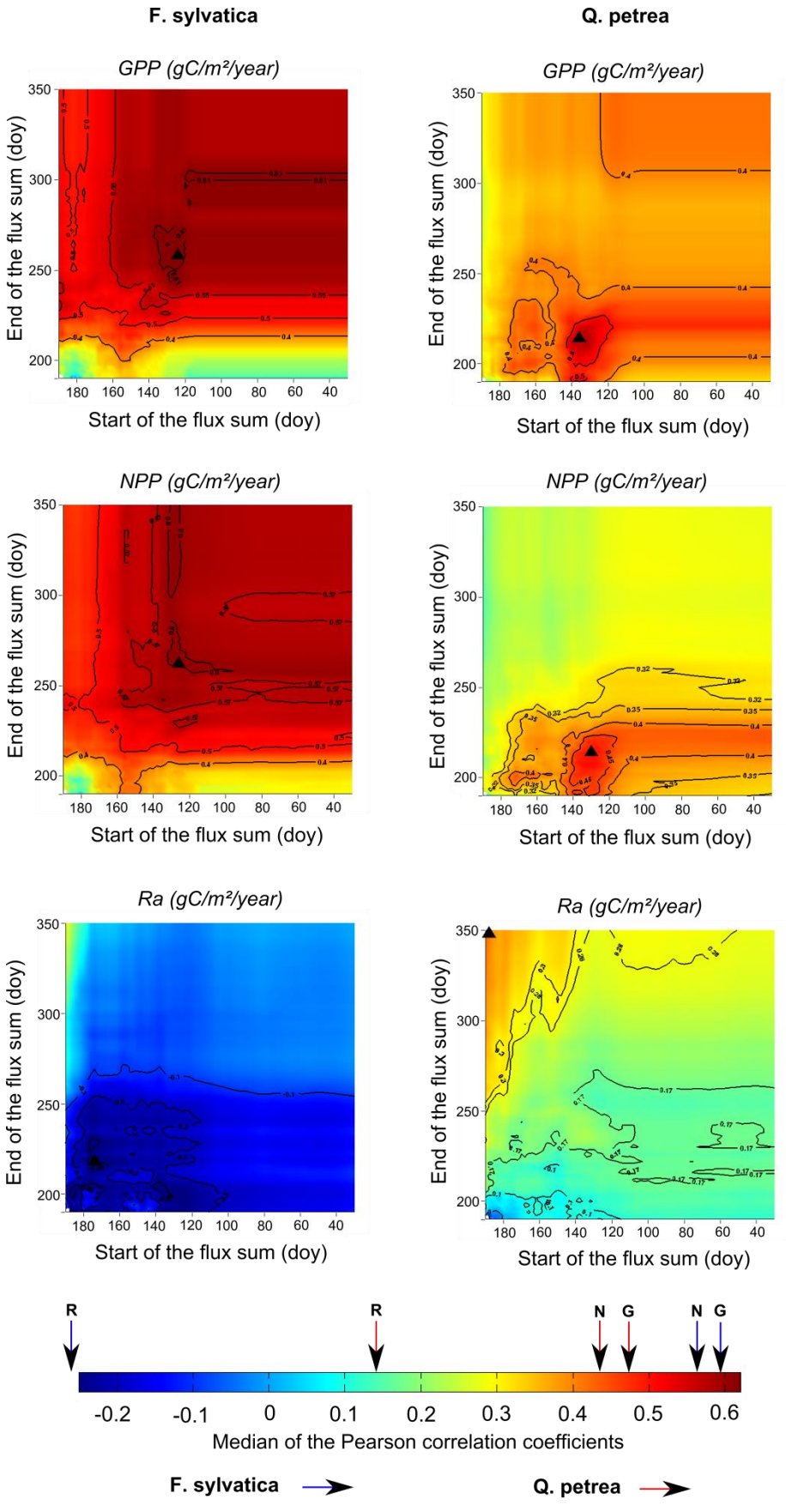
F. sylvatica
Q. petrea
GPP (gC/m²/year)
NPP (gC/m²/year)
Ra (gC/m²/year)
End of the flux sum (doy)
Start of the flux sum (doy)
350
300
250
200
180 160 140 120 100 80 60 40
R
R
N G
N G
-0.2 -0.1 0 0.1 0.2 0.3 0.4 0.5 0.6
Median of the Pearson correlation coefficients
F. sylvatica
Q. petrea

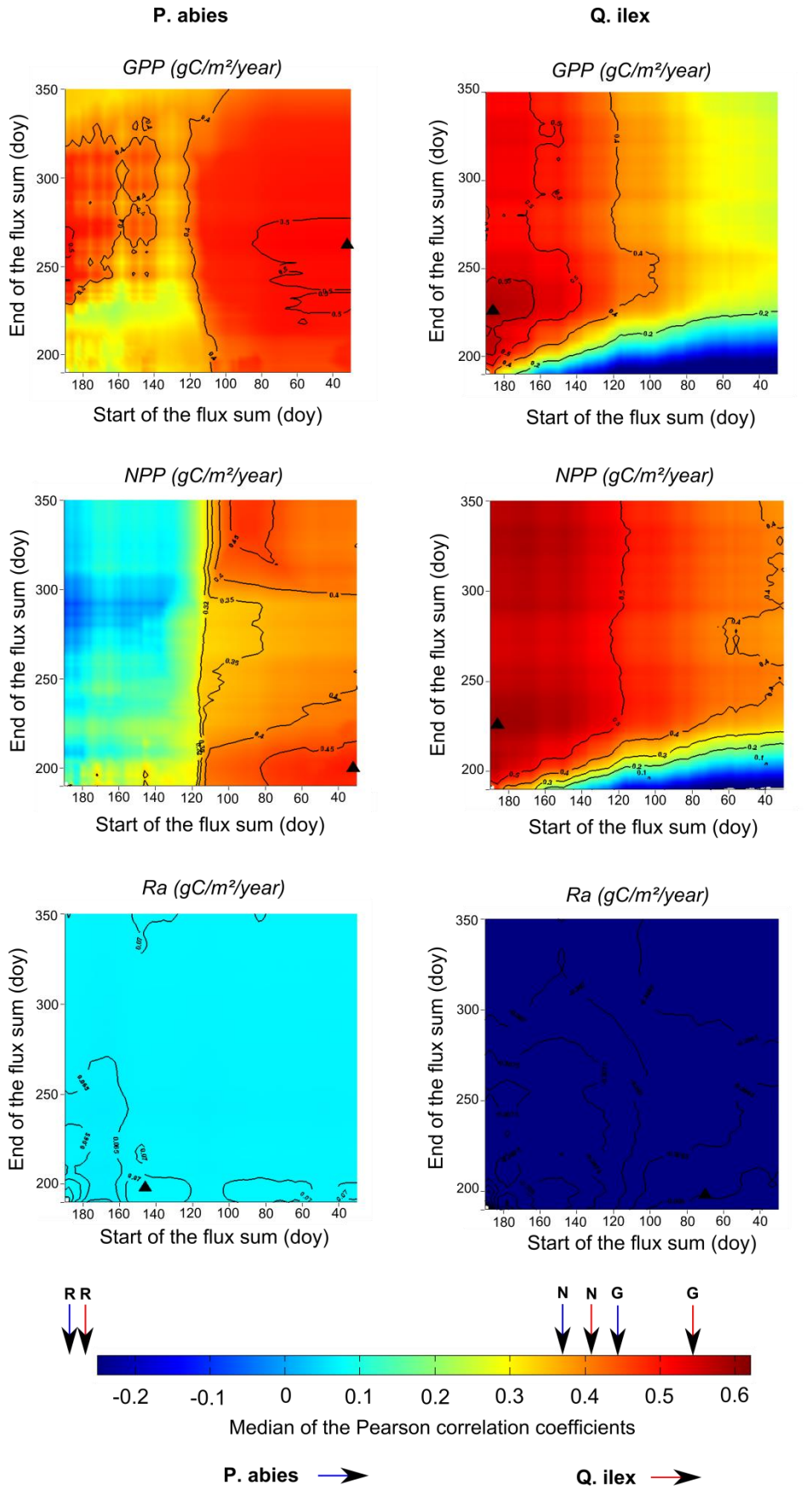
P. abies
Q. ilex
GPP (gC/m²/year)
NPP (gC/m²/year)
Ra (gC/m²/year)
End of the flux sum (doy)
Start of the flux sum (doy)
350
300
250
200
180 160 140 120 100 80 60 40
R R
N N G
G
-0.2 -0.1 0 0.1 0.2 0.3 0.4 0.5 0.6
Median of the Pearson correlation coefficients
P. abies
Q. ilex

The period we retained for the aggregation of C fluxes in the present studies was based on reported measurement on species-specific wood growth phenology (Table S8).

Table S8. Aggregation periods of carbon fluxes. Values are day of the year.

Species	Start	End	Reference
F. sylvatica	110	270	Skomarkova *et al.* 2006
Q. petraea	90	260	Michelot *et al.* 2012
P. abies	100	300	*H. Cuny, C. Rathgeber, unpublished data*
Q. ilex	130	330	*N. Martin-StPaul, unpublished data*

S7. Physiology-based index of stress water intensity

The CASTANEA model simulates daily the soil water balance, based on a bucket soil sub-model with 2 layers (a top soil layer and a total soil layer, including top soil layer) (Dufrêne et al., 2005). Based on the soil water balance, an index of water stress (reduc, unitless) is calculated daily.

$$reduc_t = \max(0, \min(1, \frac{SWC_t - SWC_{wilt}}{0.4 \times SWC_{fc}})) \qquad \text{(Eq. S18)}$$

where SWC_t is the soil water content of day t (mm), SWC_{wilt} is the soil water content at wilting point (mm) and SWC_{fc} is the soil water content at field capacity (mm).

reduc calculation is based on the water stress effect on stomatal conductance (Granier *et al.* 1999).

In addition,

$$reduc_t = 1 \text{ if } SWCtop_t > SWCtopwilt \qquad \text{(Eq. S19)}$$

where $SWCtop_t$ is the soil water content of the top soil layer (mm) and $SWCtop_{wilt}$ is the soil water content of the top soil layer at wilting point (mm). This aims to reproduce the positive effect of light rain (only affecting top soil water balance) on stomatal conductance (Dufrêne et al., 2005).

Finally,

$$\text{WS\_int} = \sum (1 - reduc_t) \qquad \text{(Eq. S20)}$$

where WS_int (unitless) is the physiology-based soil water stress intensity index. In the present study, AWBI has been related to the soil water intensity index summed over the growing period (*WS_int(n)*) and to the to the soil water intensity index summed over the previous year (*WS_int(n-1)*).

S8. Modelling of the biomass growth onset

The growth resumption of *F. sylvatica* is known to occur simultaneously with budburst (Michelot *et al.* 2012) and we simulated consequently the day of growth biomass onset for this species based on the leaf phenology sub-model of CASTANEA (Dufrêne *et al.* 2005).

For the other species, the day of growth cambial onset was simulated annually using a simple model based on daily temperature and thermic threshold (Rossi *et al.* 2008, 2011).

In this model a thermic forcing variable R_f is calculated daily as follows.

$$R_f(N) = \begin{cases} T \; if \; T(N) \geq T_b \\ 0 \; if \; T(N) < T_b \end{cases} \quad \text{(Eq. S21)}$$

where N is the day of the year, T is the daily average temperature and T_b is a threshold parameter.

Then,

$$\begin{cases} S_f(n) = \sum_{N_{start}}^{N} R_f(n) \quad if \quad S_f(n) < T_{crit} \\ D_{start} = N \quad if \quad S_f(n) = T_{crit} \end{cases} \quad \text{(Eq. S22)}$$

where S_f is a sum of temperature, T_{crit} and N_{start} are parameters and D_{start} is the day of growth onset. Species-specific parameterization of the growth biomass onset model can be found in Table S9.

Table S9. Parameterization of the biomass growth onset model.

Species	T_b	N_{start}	T_{crit}	Reference
Q. petraea	1	51	267	*A. David, N. Delpierre, unpublished data*
P. abies	-2	87	403.9	*N. Delpierre, unpublished data*
Q. ilex	5	1	933	*N. Martin-StPaul, unpublished data*

S9. Uncertainty of the CASTANEA simulations of carbon fluxes

The capacity of the CASTANEA model to reproduce annual forest C balance has been thoroughly evaluated over Europe (Delpierre 2009). We reported in Table S10 the species-specific root mean square error used in the bootstrapp procedure to account for the simulation uncertainty in linear model tests.

Table S10. Root mean square error (RMSE) of the CASTANEA simulations (Delpierre 2009)**.** GPP: gross primary productivity, Ra: autotrophic respiration, NPP: net primary productivity.

		Species			
		F. sylvatica	*Q. petraea*	*P. abies*	*Q. ilex*
RMSE ($gC.m^{-2}$)	GPP	78	104	85	88
	Ra	96	186	201	131
	NPP	60	140	66	59

References

Bergès, L., Nepveu, G. & Franc, A. (2008) Effects of ecological factors on radial growth and wood density components of sessile oak (Quercus petraea Liebl.) in Northern France. *Forest Ecology and Management*, **255**, 567–579.

Bontemps, J.-D., Hervé, J.-C. & Dhôte, J.-F. (2009) Long-term changes in forest productivity: a consistent assessment in even-aged stands. *Forest Science*, **55**, 549–564.

Bontemps, J.-D., Herve, J.-C., Duplat, P. & Dhôte, J.-F. (2012) Shifts in the height-related competitiveness of tree species following recent climate warming and implications for tree community composition: the case of common beech and sessile oak as predominant broadleaved species in Europe. *Oikos*, **121**, 1287–1299.

Bouriaud, O., Bréda, N., Le Moguédec, G. & Nepveu, G. (2004) Modelling variability of wood density in beech as affected by ring age, radial growth and climate. *Trees - Structure and Function*, **18**, 264–276.

Deleuze, C., Pain, O., Dhôte, J.F. & Hervé, J.C. (2004) A flexible radial increment model for individual trees in pure even-aged stands. *Annals of Forest Science*, **61**, 327–335.

Delpierre, N. (2009) *Etude Du Déterminisme Des Variations Interannuelles Des Échanges Carbonés Entre Les Écosystèmes Forestiers Européens et L'atmosphère : Une Approche Basée Sur La Modélisation Des Processus*. Université Paris-Sud.

Dhôte, J.-F. & Hercé, É. de. (1994) Un modèle hyperbolique pour l'ajustement de faisceaux de courbes hauteur-diamètre. *Canadian Journal of Forest Research*, **24**, 1782–1790.

Dufrêne, E., Davi, H., Francois, C., Le Maire, G., Le Dantec, V. & Granier, A. (2005) Modelling carbon and water cycles in a Beech forest. Part I: Model description and uncertainty analysis on modelled NEE. *Ecological Modelling*, **185**, 407–436.

Fritts, H.C. (2012) *Tree Rings and Climate*. Elsevier.

Genet, H., Bréda, N. & Dufrêne, E. (2010) Age-related variation in carbon allocation at tree and stand scales in beech (Fagus sylvatica L.) and sessile oak (Quercus petraea (Matt.) Liebl.) using a chronosequence approach. *Tree physiology*, **30**, 177–92.

Granier, A., Bréda, N., Biron, P. & Villette, S. (1999) A lumped water balance model to evaluate duration and intensity of drought constraints in forest stands. *Ecological Modelling*, **116**, 269–283.

Guillemot, J., Delpierre, N., Vallet, P., François, C., Martin-StPaul, N.K., Soudani, K., Nicolas, M., Badeau, V. & Dufrêne, E. (2014) Assessing the effects of management on forest growth across France: insights from a new functional–structural model. *Annals of Botany*, doi: 10.1093/aob/mcu059.

Guilley, E., Hervé, J.-C. & Nepveu, G. (2004) The influence of site quality, silviculture and region on wood density mixed model in Quercus petraea Liebl. *Forest Ecology and Management*, **189**, 111–121.

Lebourgeois, F. (1997) RENECOFOR - Etude dendrochronologique des 102 peuplements du réseau. *Office national des forêts, Département des recherches techniques*.

Lehtonen, a, Mäkipää, R., Heikkinen, J., Sievänen, R. & Liski, J. (2004) Biomass expansion factors (BEFs) for Scots pine, Norway spruce and birch according to stand age for boreal forests. *Forest Ecology and Management*, **188**, 211–224.

Michelot, A., Simard, S., Rathgeber, C., Dufrêne, E. & Damesin, C. (2012) Comparing the intra-annual wood formation of three European species (Fagus sylvatica, Quercus petraea and Pinus sylvestris) as related to leaf phenology and non-structural carbohydrate dynamics. *Tree physiology*, **32**, 1033–45.

Pignard, G., Dupouey, J., Arrouays, D. & Loustau, D. (2000) Carbon stocks estimates for French forests. *Biotechnol. Agron. Soc. Environ.*, **4**, 285–289.

Rambal, S., Joffre, R., Ourcival, J.M., Cavender-Bares, J. & Rocheteau, A. (2004) The growth respiration component in eddy CO2 flux from a Quercus ilex mediterranean forest. *Global Change Biology*, **10**, 1460–1469.

Rossi, S., Deslauriers, A., Griçar, J., Seo, J., Rathgeber, C.B.K., Anfodillo, T., Morin, H., Levanic, T., Oven, P. & Jalkanen, R. (2008) Critical temperatures for xylogenesis in conifers of cold climates. *Global Ecology and Biogeography*, **17**, 696–707.

Rossi, S., Morin, H., Deslauriers, A. & Plourde, P.-Y. (2011) Predicting xylem phenology in black spruce under climate warming. *Global change biology*, **17**, 614–625.

Seynave, I., Gégout, J., Hervé, J., Drapier, J., Bruno, É. & Dumé, G. (2005) Picea abies site index prediction by environmental factors and understorey vegetation : a two-scale approach based on survey databases. , **1678**, 1669–1678.

Skomarkova, M. V., Vaganov, E. a., Mund, M., Knohl, a., Linke, P., Boerner, a. & Schulze, E.-D. (2006) Inter-annual and seasonal variability of radial growth, wood density and carbon isotope ratios in tree rings of beech (Fagus sylvatica) growing in Germany and Italy. *Trees*, **20**, 571–586.

Vallet, P., Dhôte, J.-F., Moguédec, G. Le, Ravart, M. & Pignard, G. (2006) Development of total aboveground volume equations for seven important forest tree species in France. *Forest Ecology and Management*, **229**, 98–110.

Wilhelmsson, L., Arlinger, J., Spångberg, K., Lundqvist, S.-O., Grahn, T., Hedenberg, Ö. & Olsson, L. (2002) Models for Predicting Wood Properties in Stems of Picea abies and Pinus sylvestris in Sweden. *Scandinavian Journal of Forest Research*, **17**, 330–350.

Zhang, S.-Y., Owoundi, R.E., Nepveu, G., Mothe, F. & Dhôte, J.-F. (1993) Modelling wood density in European oak (Quercuspetraea and Quercusrobur) and simulating the silvicultural influence. *Canadian Journal of Forest Research*, **23**, 2587–2593.